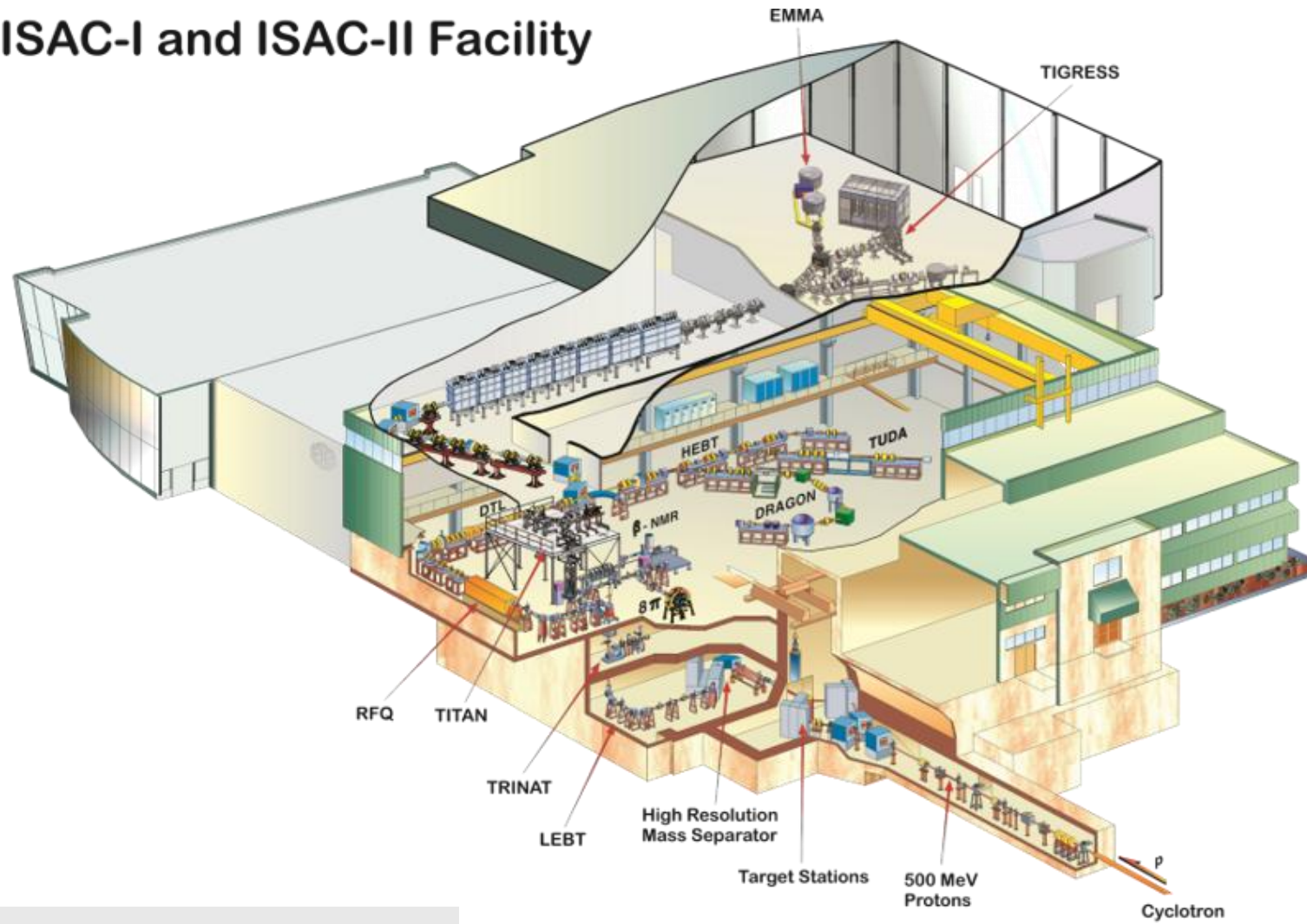


Outline

- **TRIUMF: an ISOL facility in Vancouver, Canada**
- **Multiple-Reflection Time-of-Flight mass spectrometry (MR-TOF-MS)**
- **Study the 1st and 2nd *r*-process peaks**
- **High-precision mass measurements of Ga and Zn nuclei**
- **Toward the most neutron-rich Sn isotopes**

TRIUMF facility (Vancouver, Canada)

ISAC-I and ISAC-II Facility



Programs in

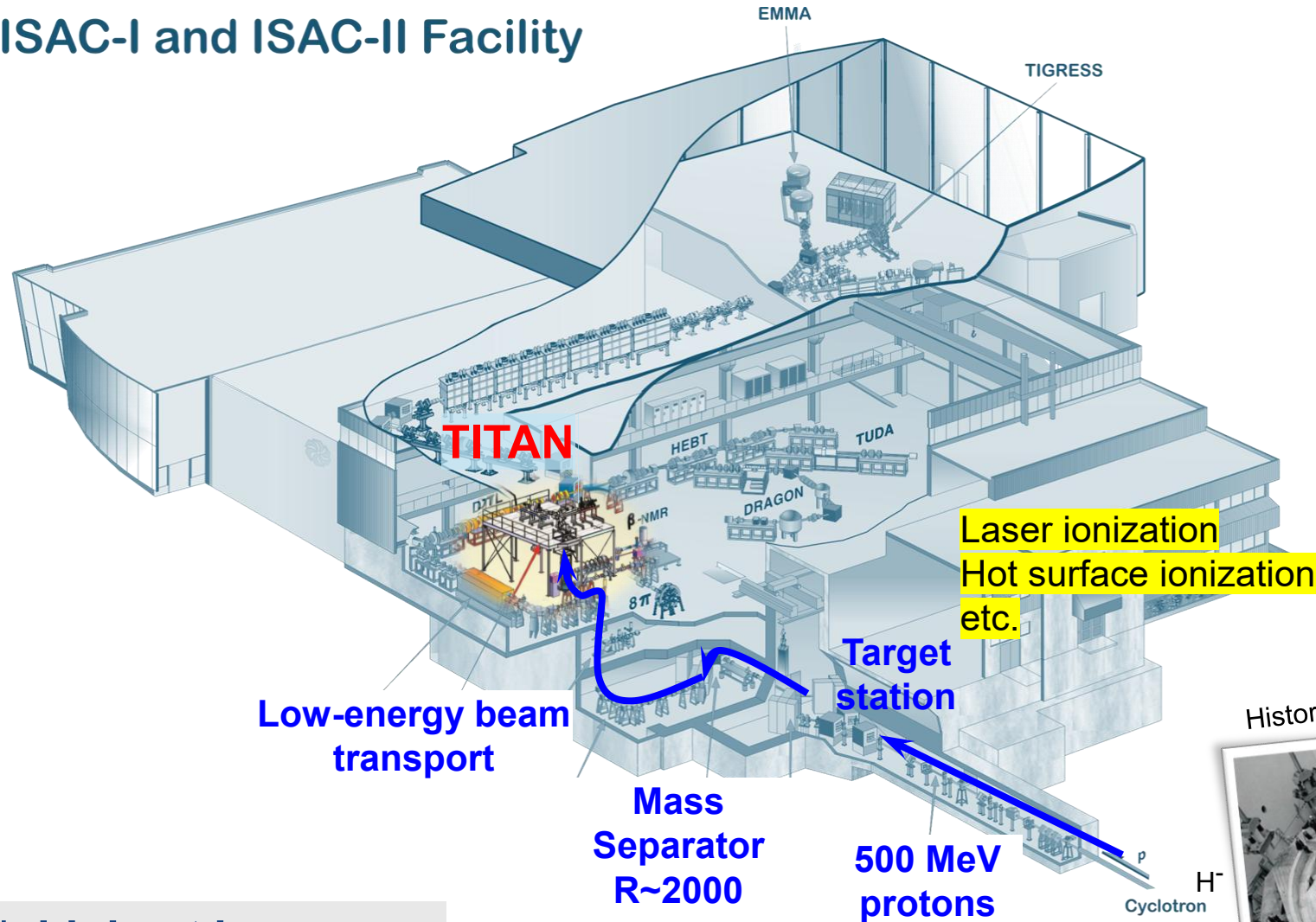
- Nuclear structure & reactions
- Nuclear astrophysics
- Electroweak interaction Studies
- Material science
- Life science

ISOL facility with **highest beam power on target (50 kW)**



TITAN at ISAC/TRIUMF

ISAC-I and ISAC-II Facility



TRIUMF's Ion Trap for Atomic and Nuclear Science

- High-precision mass measurements
- In-trap decay spectroscopy

ISOL facility with **highest beam power on target (50 kW)**



TITAN ion traps

MR-TOF-MS:
Mass measurements
Beam diagnostic & yields
RIB beam purification

RFQ:
Accumulation,
cooling, and
bunching

20 keV

hot RIB

MR-TOF

isobaric
purified
beam

RFQ cooler-buncher

cooled SCI
bunches

1.3-2.2 keV

SCI

HCI

EBIT

MPET

MPET:
Penning trap for
mass measurements

EBIT:
Charge State Breeding
and
decay spectroscopy

J. Dilling *et al.*, NIMB 204 (2003) 492,
C. Jesch *et al.*, Hyperfine Interact. 235 (2015) 97



TITAN ion traps

JUSTUS-LIEBIG-
UNIVERSITÄT
GIESSEN

MR-TOF-MS:
Mass measurements
Beam diagnostic & yields
RIB beam purification

MR-TOF-MS was developed,
built and continuously improved
by the JLU Giessen

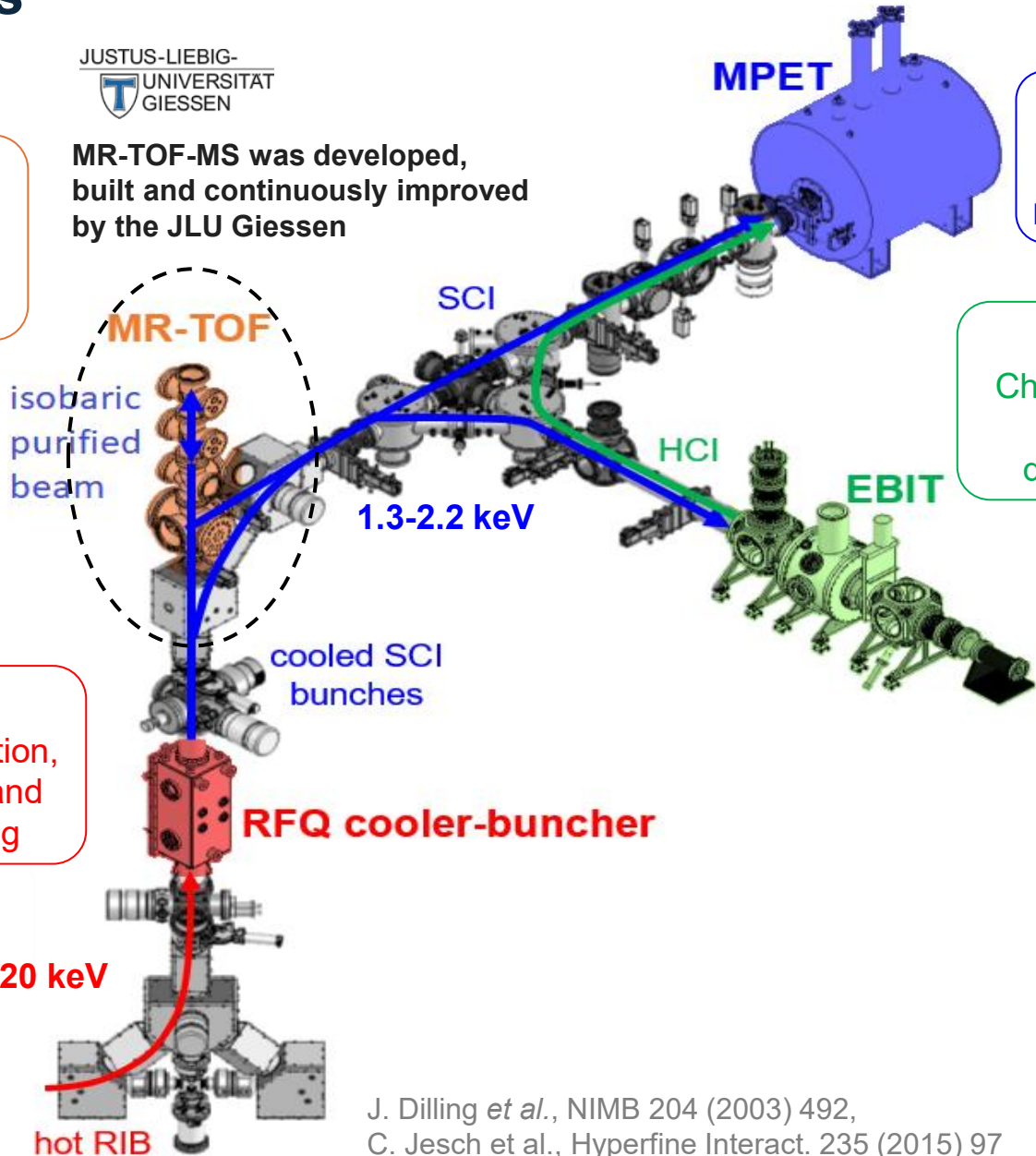
MPET:
Penning trap for
mass measurements

EBIT:
Charge State Breeding
and
decay spectroscopy

RFQ:
Accumulation,
cooling, and
bunching

20 keV

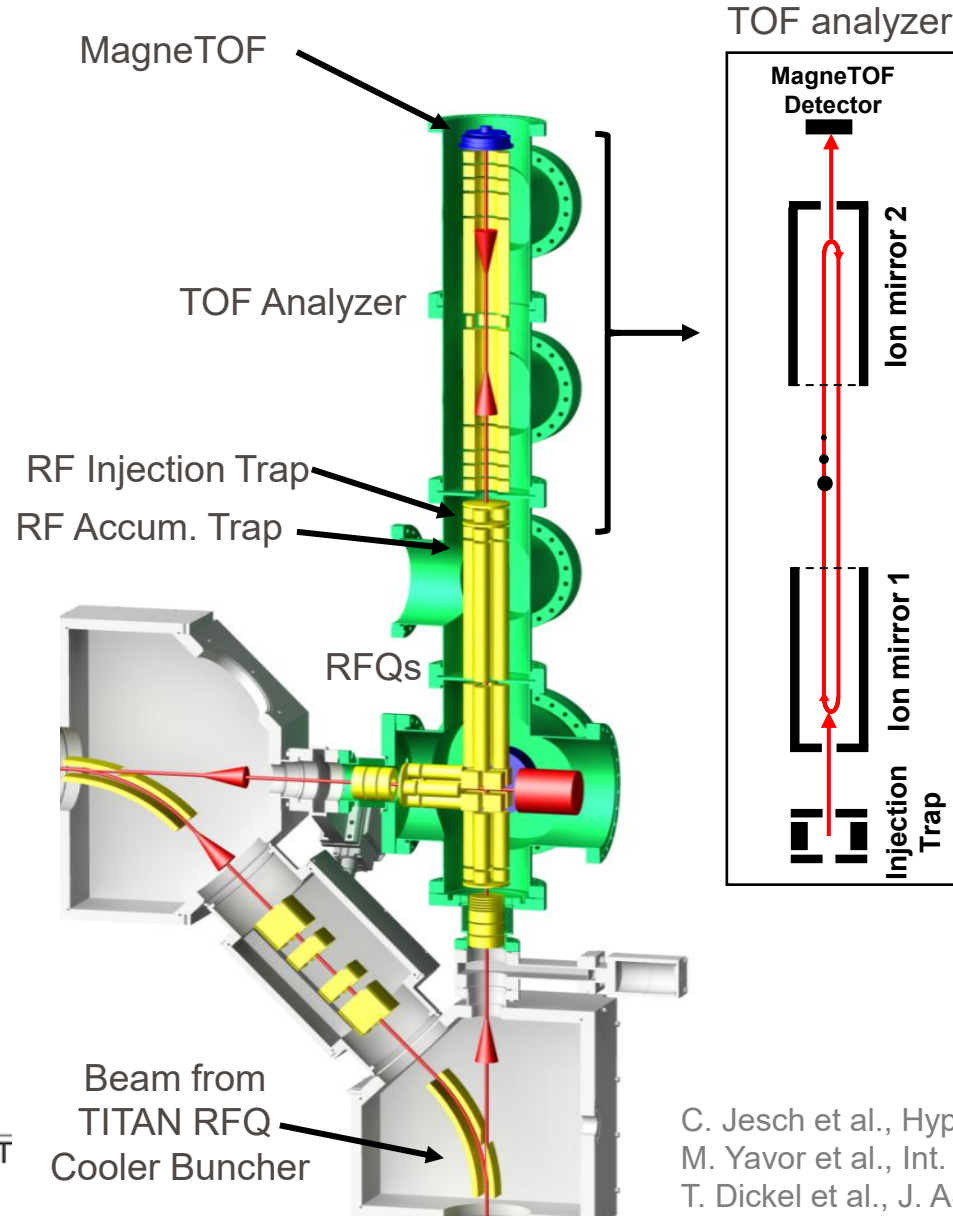
hot RIB



J. Dilling *et al.*, NIMB 204 (2003) 492,
C. Jesch *et al.*, Hyperfine Interact. 235 (2015) 97



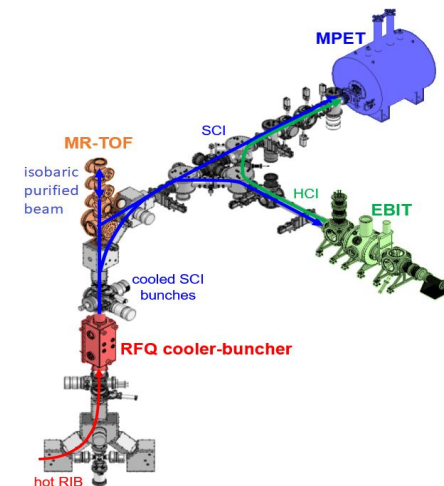
Multiple Reflection Time-Of-Flight Mass Spectrometer (MR-TOF-MS)



- Measurement of mass-to-charge ratio by measurement of time-of-flight:

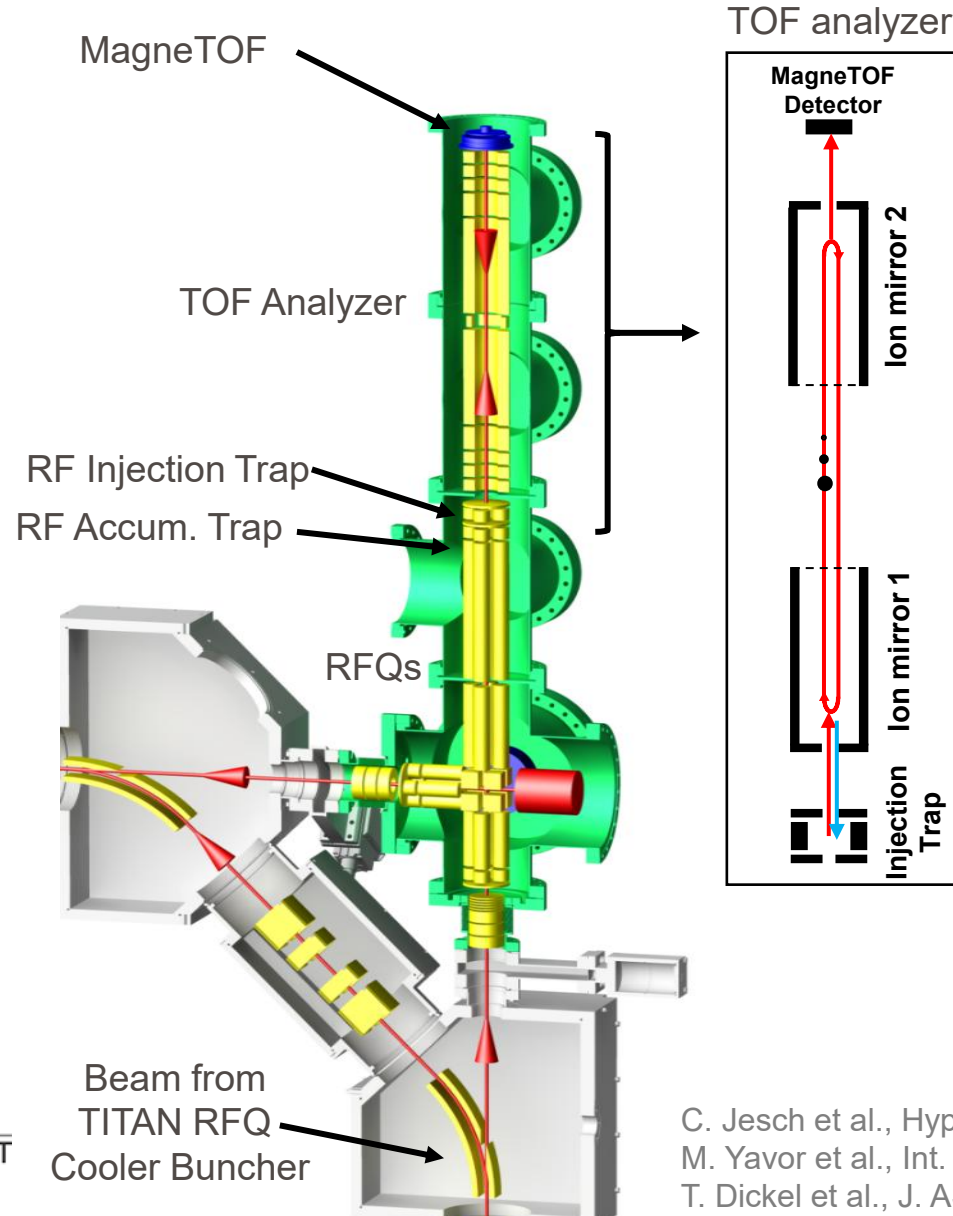
$$E = \frac{1}{2}mv^2 = qeU$$

$$\Rightarrow \frac{m}{q} \propto TOF^2$$



C. Jesch et al., Hyperfine Interact. 235 (2015) 97
 M. Yavor et al., Int. J. Mass Spec. 381 (2015) 1-9
 T. Dickel et al., J. ASMS 28 (2017) 1079

Multiple Reflection Time-Of-Flight Mass Spectrometer (MR-TOF-MS)



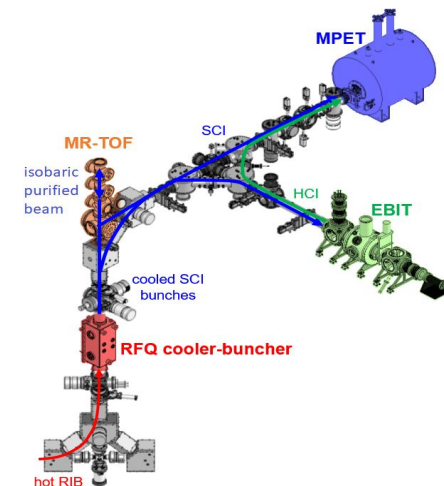
- Measurement of mass-to-charge ratio by measurement of time-of-flight:

$$E = \frac{1}{2}mv^2 = qeU$$

$$\Rightarrow \frac{m}{q} \propto TOF^2$$

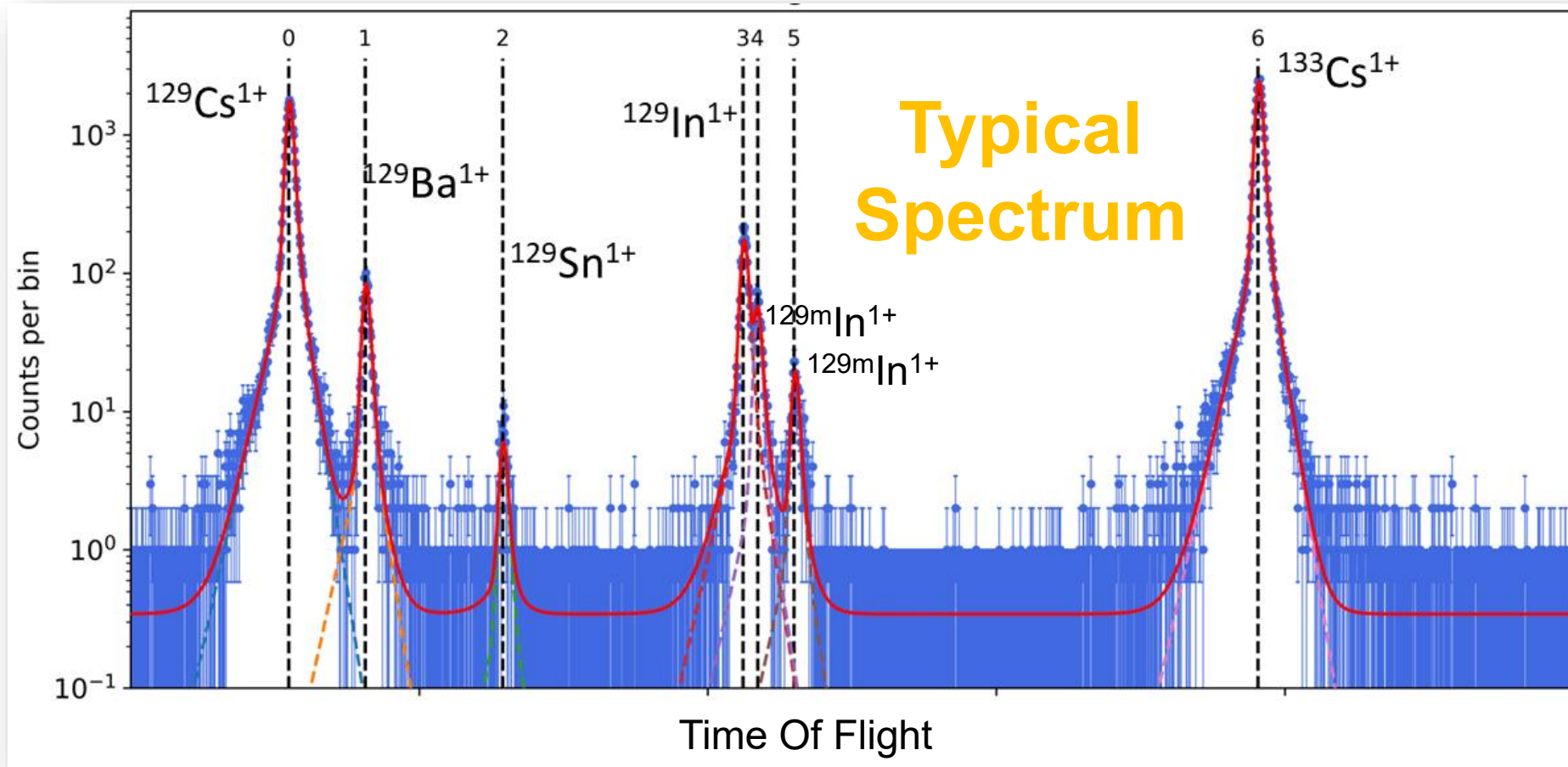
- Isobaric separator and beam purification for **itself** and **other traps**

Mass Selective Re-Trapping

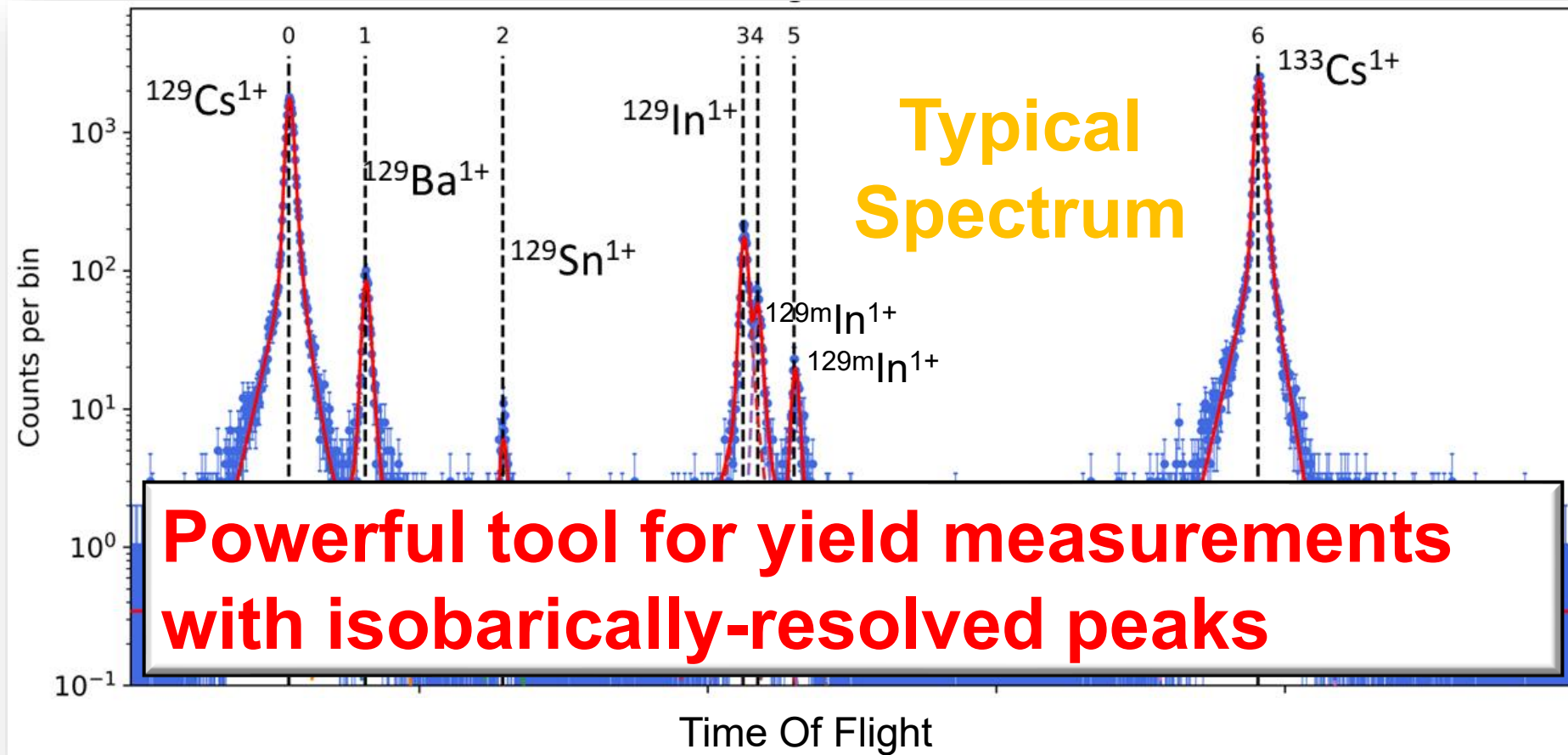


C. Jesch et al., Hyperfine Interact. 235 (2015) 97
 M. Yavor et al., Int. J. Mass Spec. 381 (2015) 1-9
 T. Dickel et al., J. ASMS 28 (2017) 1079

Multiple Reflection Time-Of-Flight Mass Spectrometer (MR-TOF-MS)

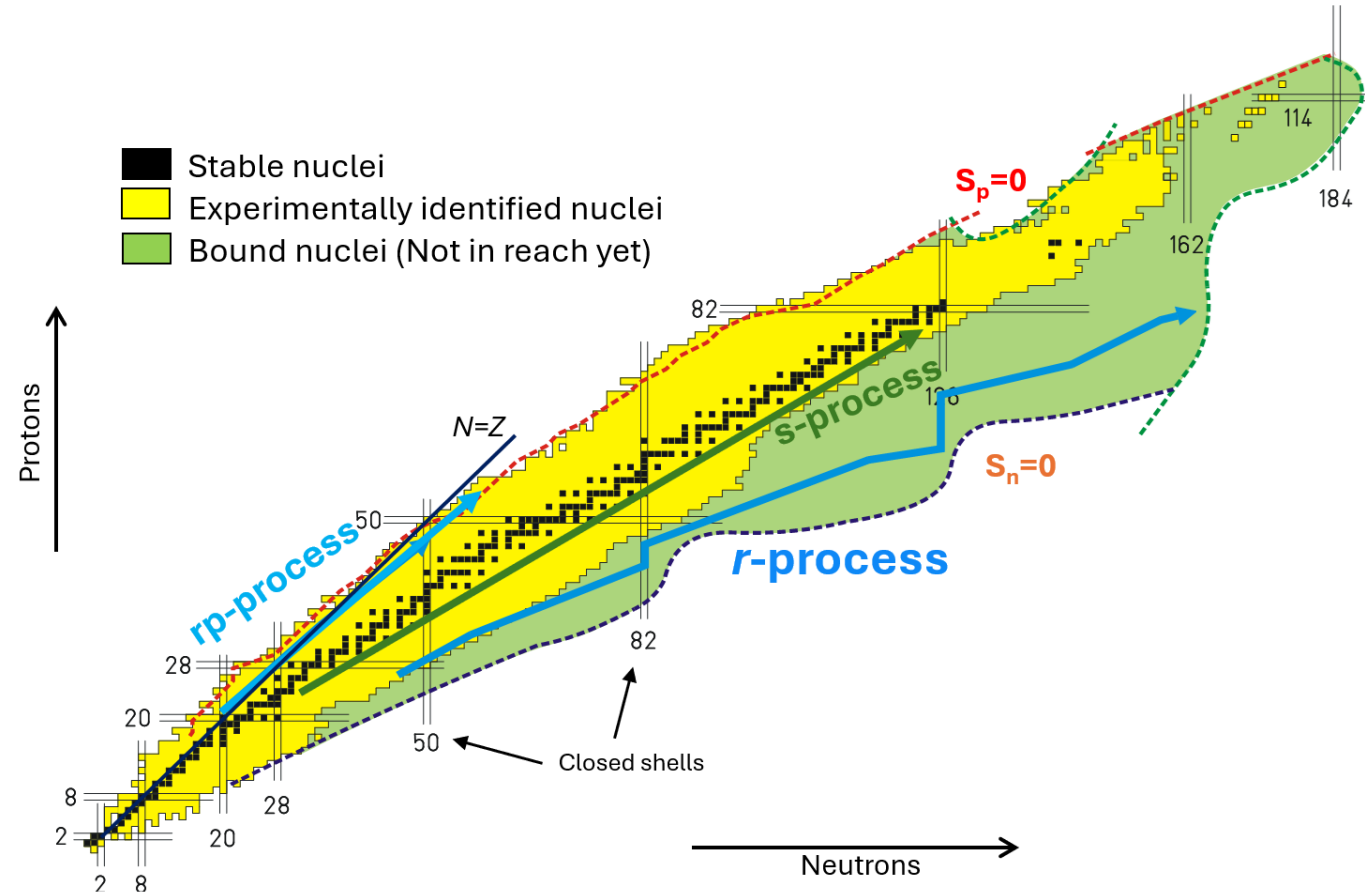


Multiple Reflection Time-Of-Flight Mass Spectrometer (MR-TOF-MS)



Production/identification of exotic nuclei

- At the limit of facilities or beyond (in-flight and ISOL productions)
- Low production cross sections, short half-lives and background contamination
- Needs for **fast** and **efficient** experimental methods

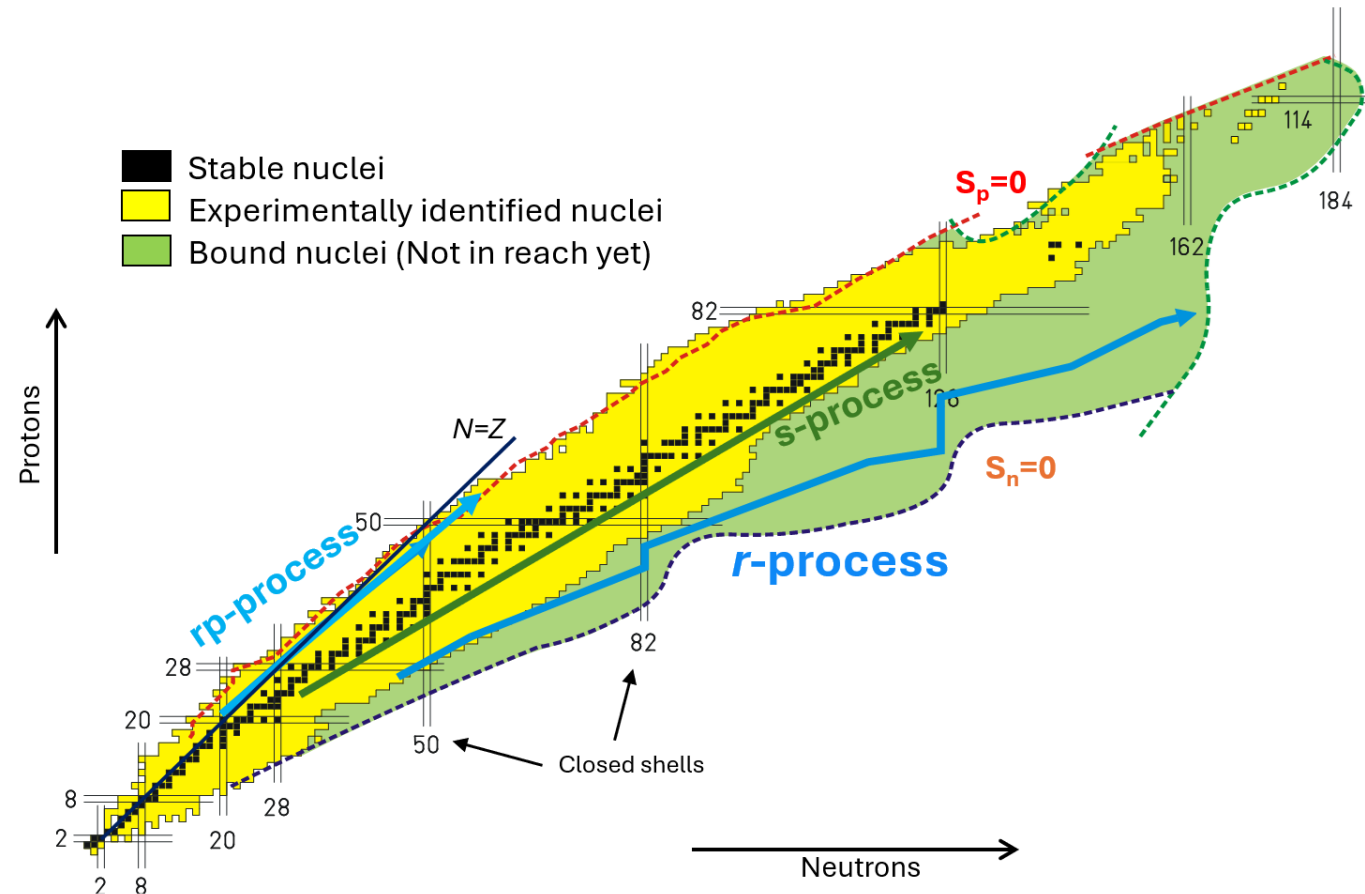


Production/identification of exotic nuclei

- At the limit of facilities or beyond (in-flight and ISOL productions)
- Low production cross sections, short half-lives and background contamination
- Needs for **fast** and **efficient** experimental methods

**** MR-TOF-MS ****

- **Non-scanning** and **Broadband** (RIB beam profile)
- Fast cycles (10s ms)
- 600k mass resolution within 15ms (#IT=1000)
- High mass accuracy 10^{-7}
- Background handling $1:10^8$
- High sensitivity 2-3 counts/h



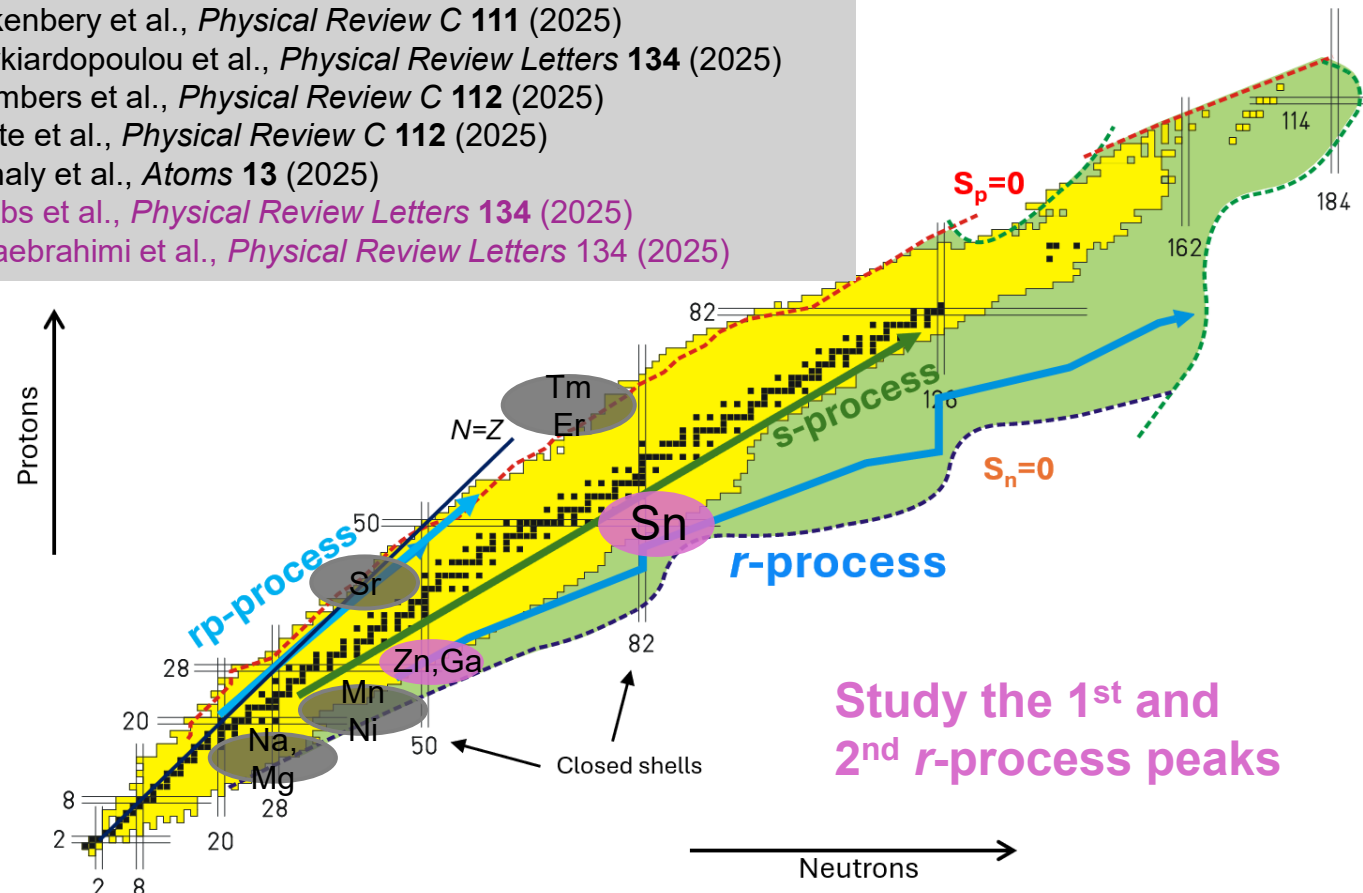
Production/identification of exotic nuclei

- At the limit of facilities or beyond (in-flight and ISOL productions)
- Low production cross sections, short half-lives and background contamination
- Needs for **fast** and **efficient** experimental methods

**** MR-TOF-MS ****

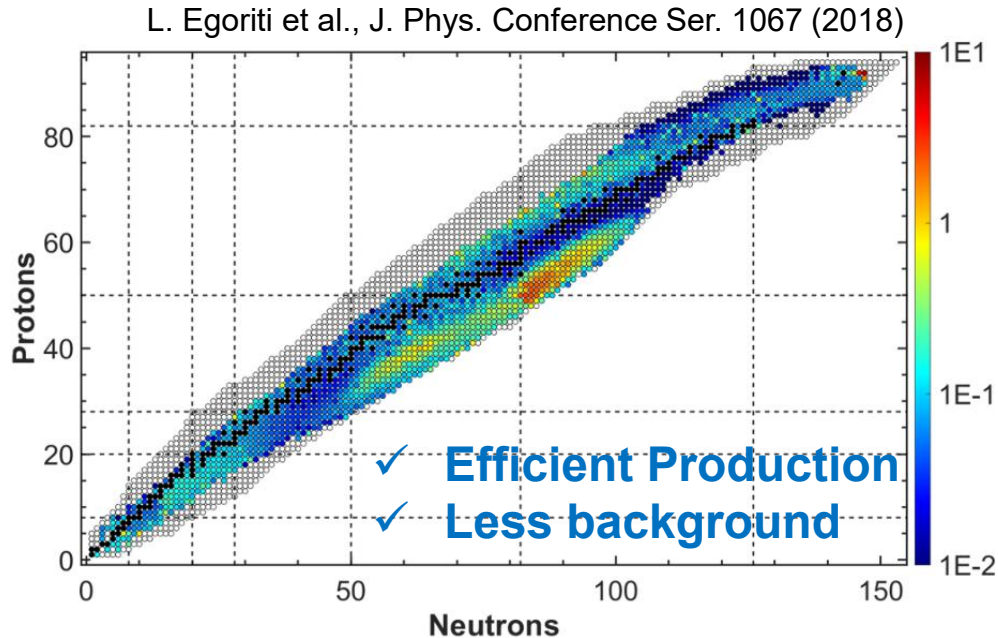
- **Non-scanning** and **Broadband** (RIB beam profile)
- Fast cycles (10s ms)
- 600k mass resolution within 15ms (#IT=1000)
- High mass accuracy 10^{-7}
- Background handling $1:10^8$
- High sensitivity 2-3 counts/h

Z. Hockenbery et al., *Physical Review C* **111** (2025)
E.M. Lykiardopoulou et al., *Physical Review Letters* **134** (2025)
C. Chambers et al., *Physical Review C* **112** (2025)
B. Kootte et al., *Physical Review C* **112** (2025)
A. Czihaly et al., *Atoms* **13** (2025)
A. Jacobs et al., *Physical Review Letters* **134** (2025)
A. Mollaebrahimi et al., *Physical Review Letters* **134** (2025)

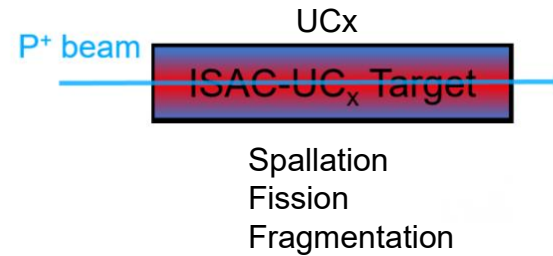
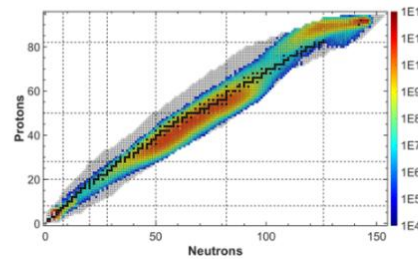


Experiments made possible thanks to the new target developments

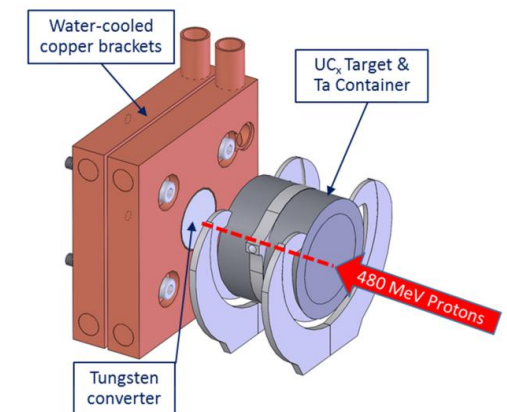
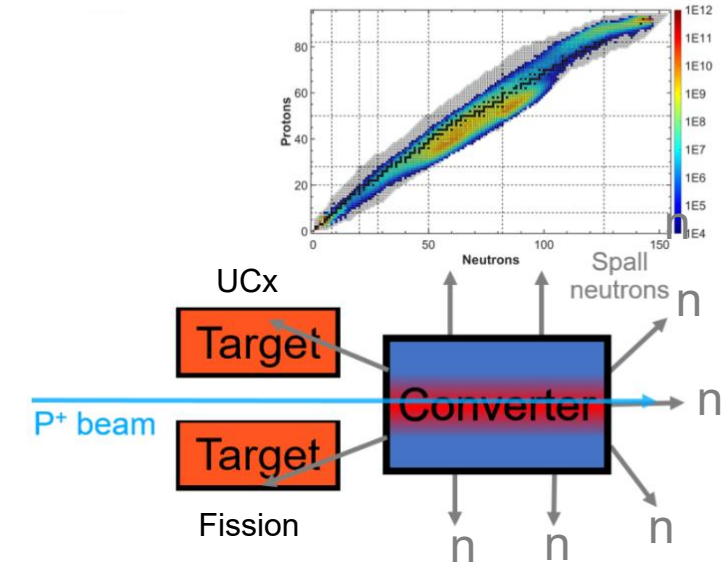
- Commissioning of the new **p-to-n target**
- Fission yields measurements (MR-TOF-MS)



Conventional Target



P-to-n Target



L. Egoriti et al., J. Phys. Conference Ser. 1067 (2018)

Neutron-rich Zn and Ga nuclei

- ✓ First mass measurement of ^{83}Zn and ^{86}Ga
- ✓ Improved precision (x3) for ^{85}Ga
- ✓ The isomer at $^{79\text{m}}\text{Zn}$ with $\text{Exc.}=941\text{ keV}$:

In agreement with [L. Nies et al., Phys. Rev. Lett. 131 (2023)]

Atomic Mass Excess (ME) of $^{79-83}\text{Zn}$ and $^{85,86}\text{Ga}$

Species	Calibrant	Mass ratio	ME _{TITAN} (keV/c ²)	ME _{AME2020} (keV/c ²)	Difference (keV/c ²)
^{79}Zn	^{79}Ga	1.000 136 781 (51)	−53 430.0 (79)	−53 432.3 (22)	2.3 (8.4)
$^{79\text{m}}\text{Zn}$	^{79}Ga	1.000 136 78 (16)	−52 491 (14)	−52 330 (150)*	161 (151)
^{80}Zn	^{80}Rb	1.000 275 561 (48)	−51 661 (10)	−51 648.6 (26)	−12 (11)
^{81}Zn	^{81}Ga	1.000 151 46 (11)	−46 209 (12)	−46 200 (5)	−9 (13)
^{82}Zn	^{82}Ga	1.000 139 116 (91)	−42 312 (10)	−42 314 (3)	2 (10)
^{83}Zn	^{83}Ga	1.000 167 56 (22)	−36 311 (18)
^{85}Ga	^{85}Rb	1.000 536 66 (15)	−39 720 (14)	−39 740 (40)	20 (42)
^{86}Ga	^{86}Rb	1.000 612 03 (23)	−33 768 (20)

A. Jacobs et al., *Physical Review Letters* 134 (2025)

Study the 1st
r-process peaks

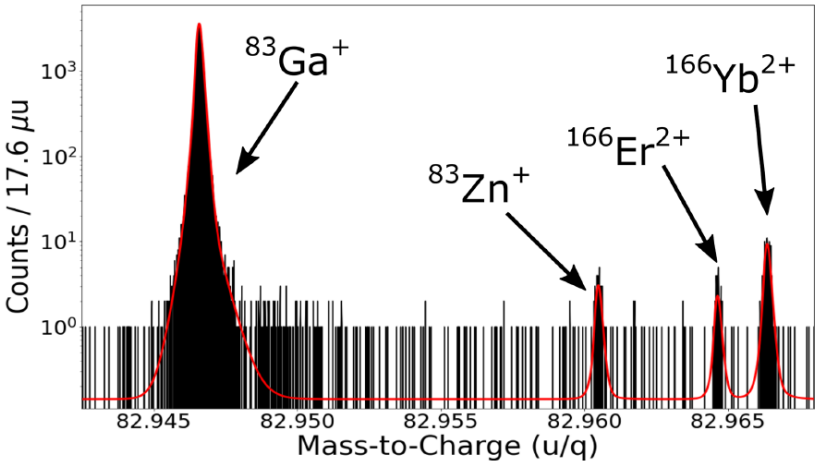
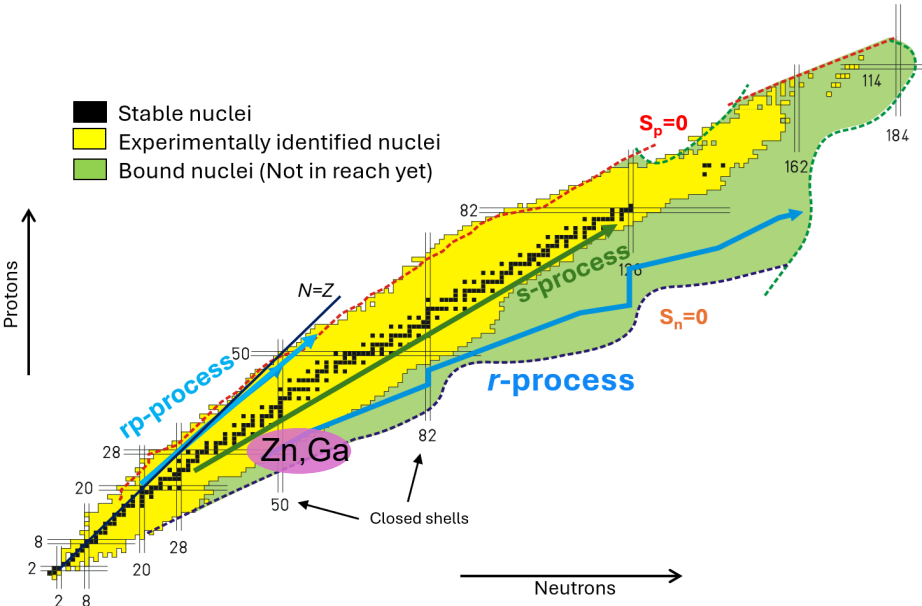
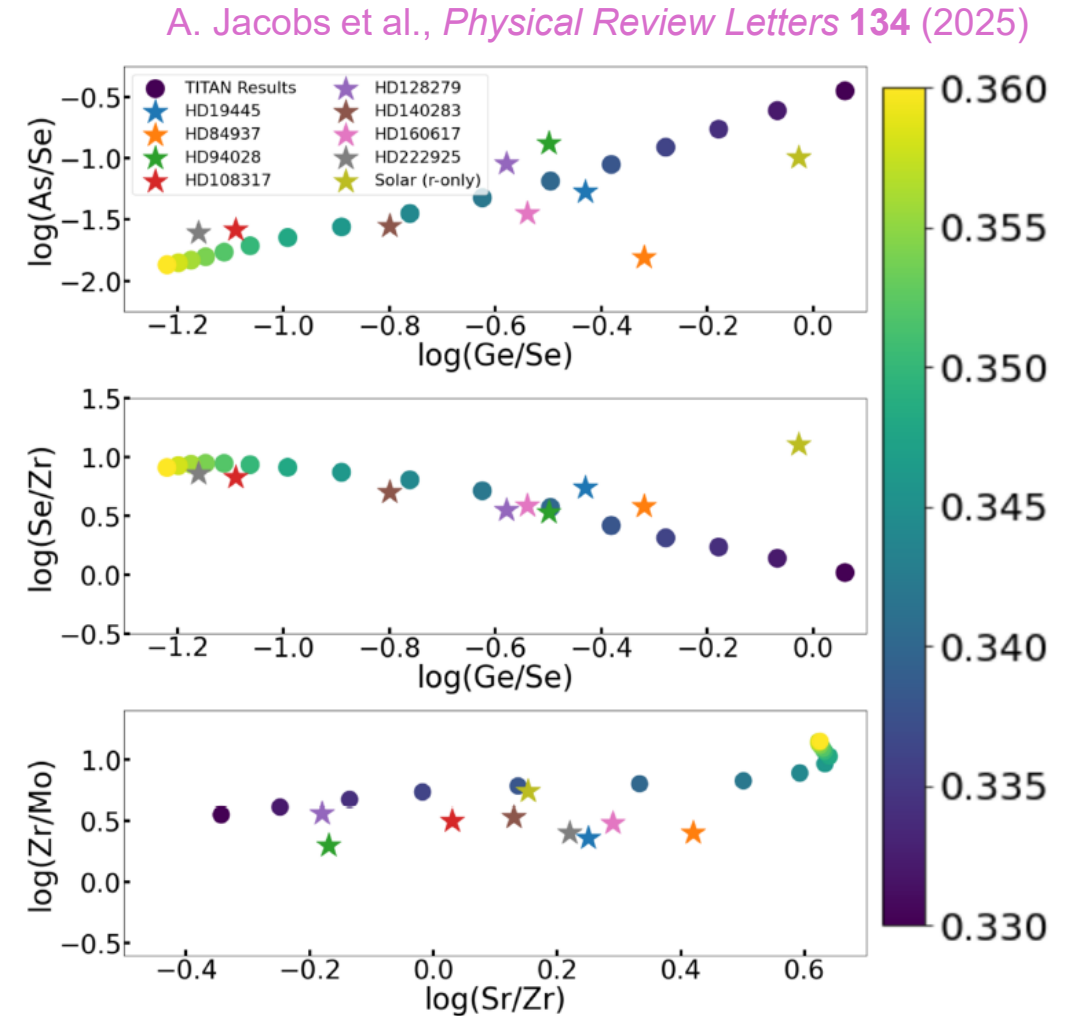
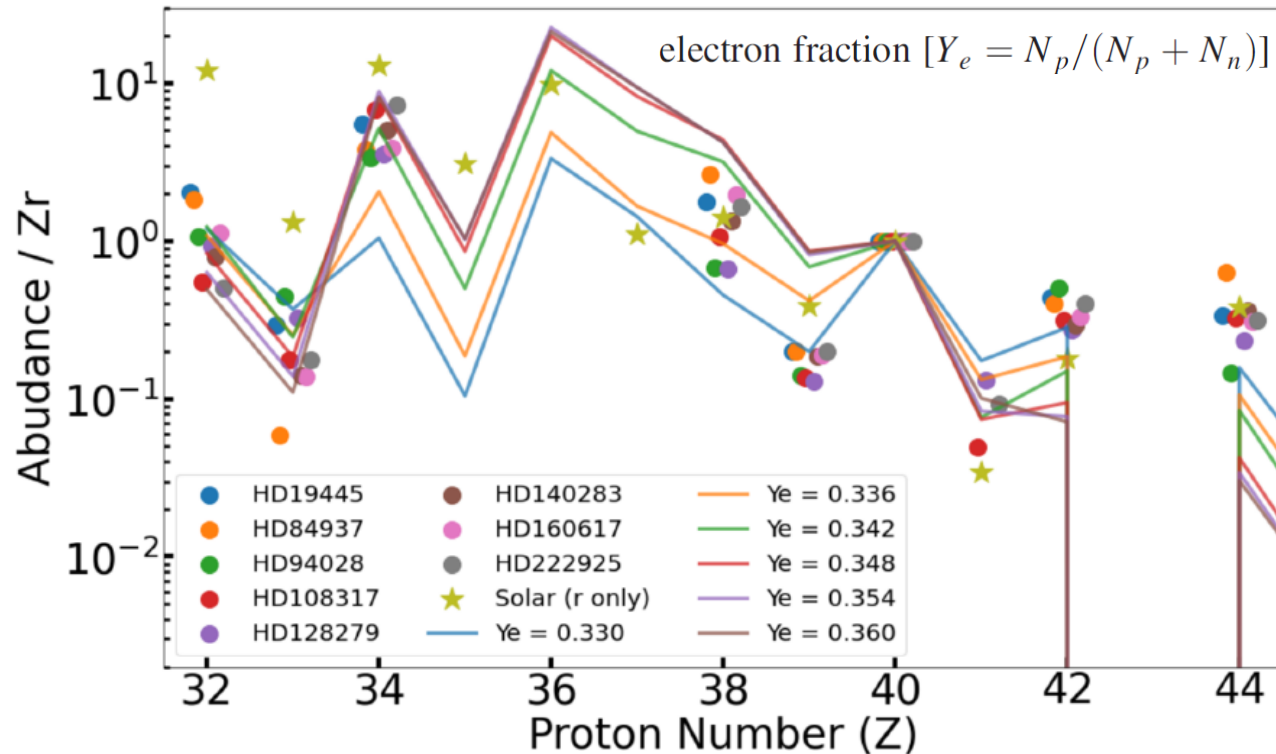


FIG. 1. The spectrum and fit (red) for $A/q = 83$ at 900 turns after 2.5 h accumulation. $^{83}\text{Ga}^+$ has been used as the calibration species.

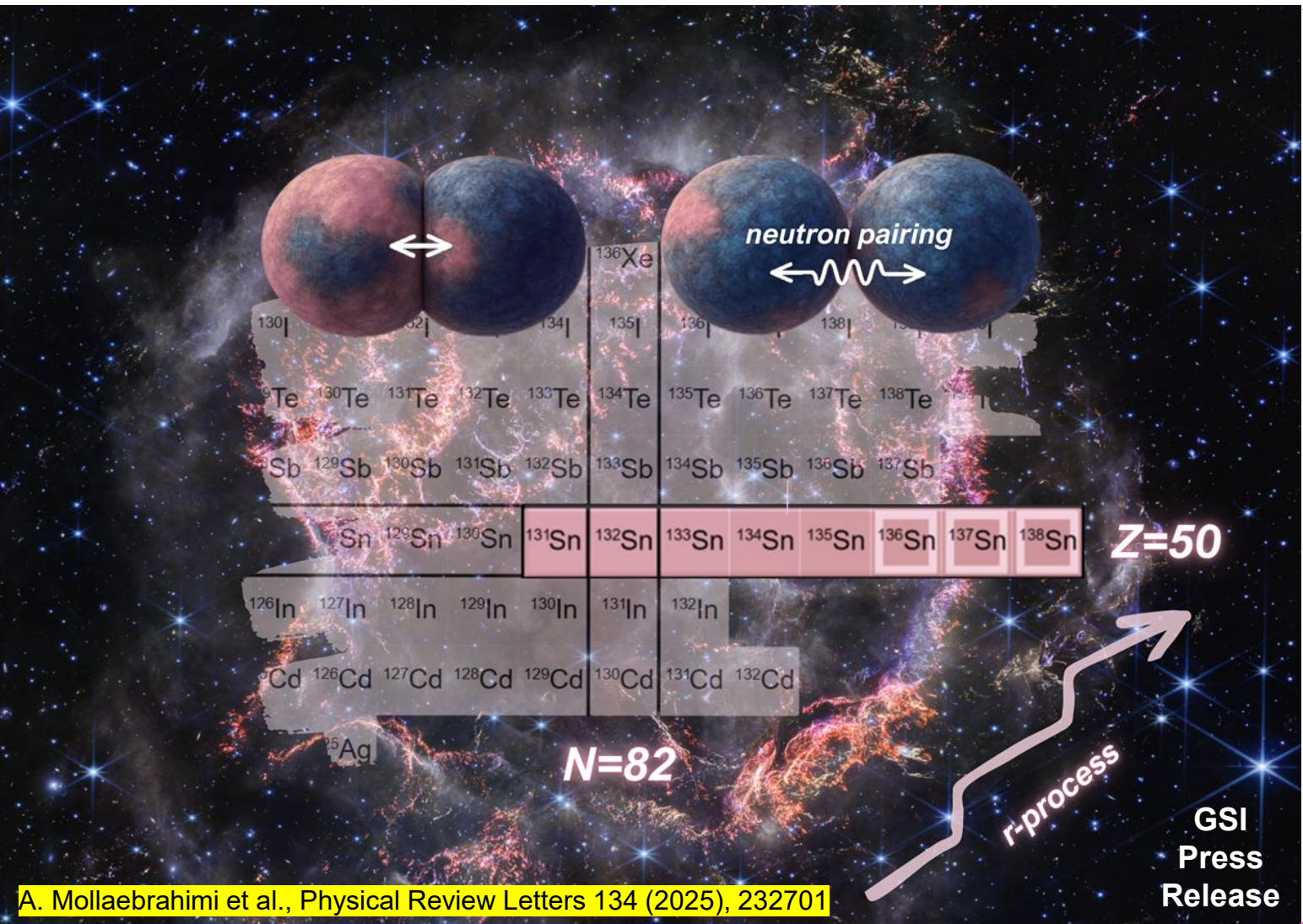


Neutron-rich Zn and Ga nuclei

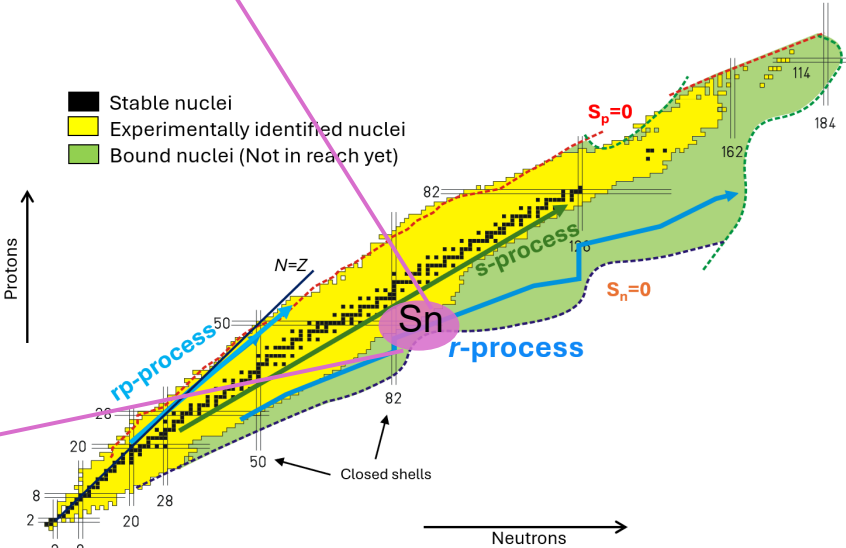
- Elemental abundances for Solar and other stars
- Different astrophysical conditions [Ye], expected range for a binary neutron star (BNS) mergers
- High sensitivity on the Ye of BNS merger near 1st r-process peak
- By varying the Ye, we can reproduce the abundance of several metal-poor (old) stars → question the need for i-process
- By varying the Ye, we reproduce the correlations between key elemental ratios



Mass measurements of the neutron-rich Sn isotopes



Impact on the 2nd *r*-process peak



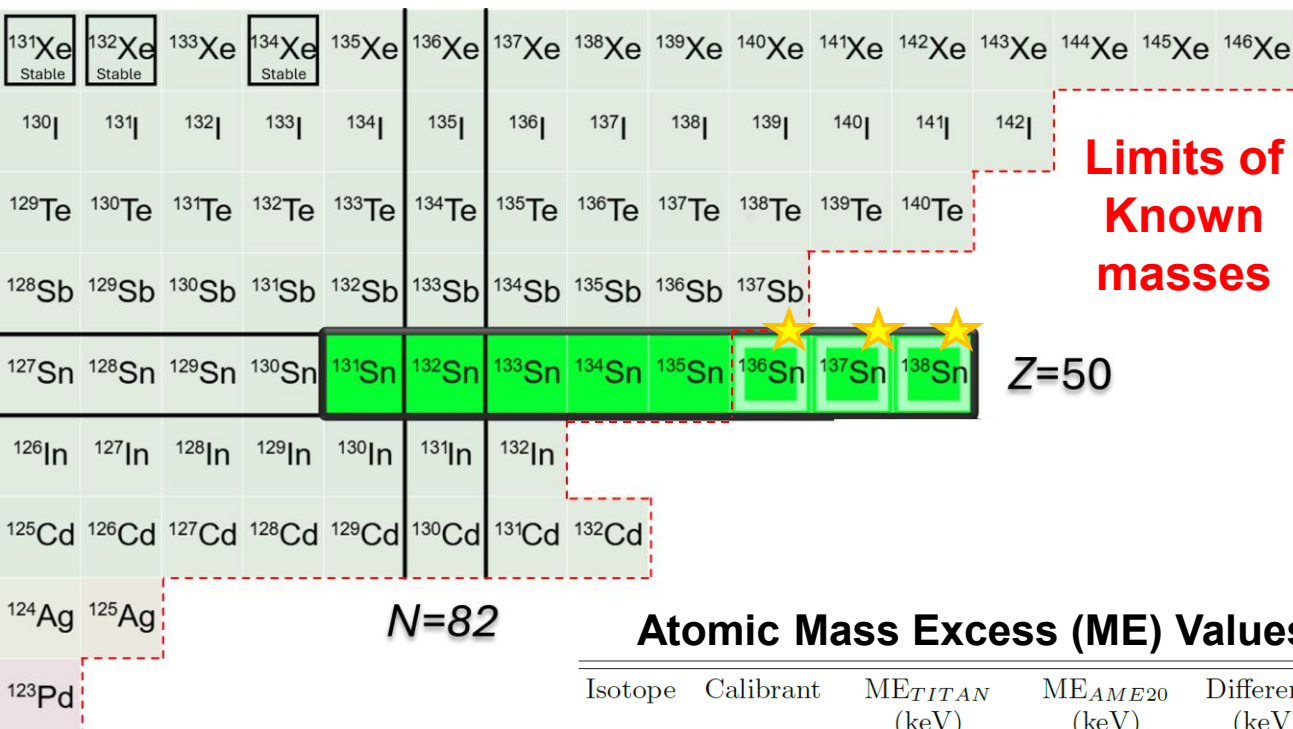
A. Mollaebrahimi et al., Physical Review Letters 134 (2025), 232701

NASA, ESA, CSA, STScI, Danny Milisavljevic (Purdue University), Ilse De Looze (UGhent), Tea Temim (Princeton University). AI tools were used to generate the image.

Neutron-rich Sn isotopes

- First time mass measurements of $^{136-138}\text{Sn}$ isotopes

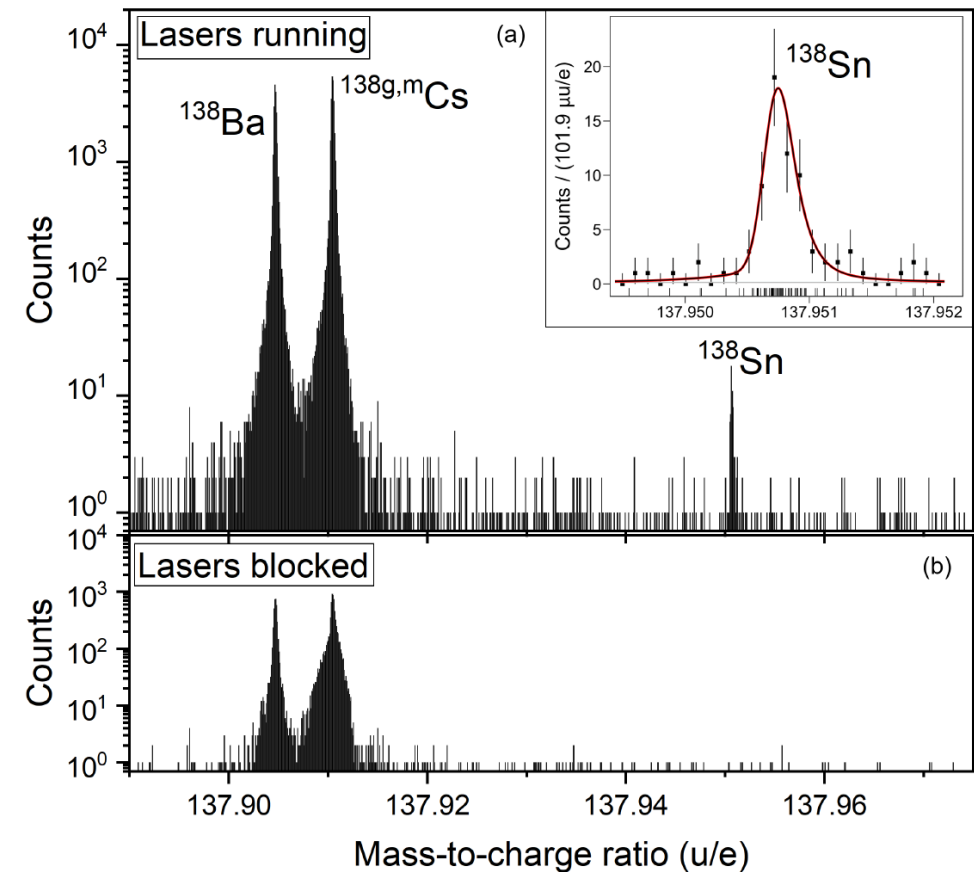
A. Mollaebrahimi et al., Physical Review Letters 134 (2025), 232701



Atomic Mass Excess (ME) Values

Isotope	Calibrant	ME _{TITAN} (keV)	ME _{AME20} (keV)	Difference (keV)
^{131}Sn	^{131}Cs	-77268 ± 22	-77265 ± 4	-3 ± 23
^{132}Sn	^{132}Cs	-76539 ± 11	-76547 ± 2	7 ± 11
^{133}Sn	^{133}Cs	-70870 ± 24	-70874 ± 2	4 ± 24
^{134}Sn	^{134}Ba	-66445 ± 26	-66434 ± 3	-11 ± 27
^{135}Sn	^{135m}Cs	-60647 ± 15	-60632 ± 3	-15 ± 15
^{136}Sn	^{136}Ba	-56074 ± 29
^{137}Sn	^{137}Cs	-50110 ± 10
^{138}Sn	^{138}Ba	-45442 ± 21

Identification by mass and Lasers

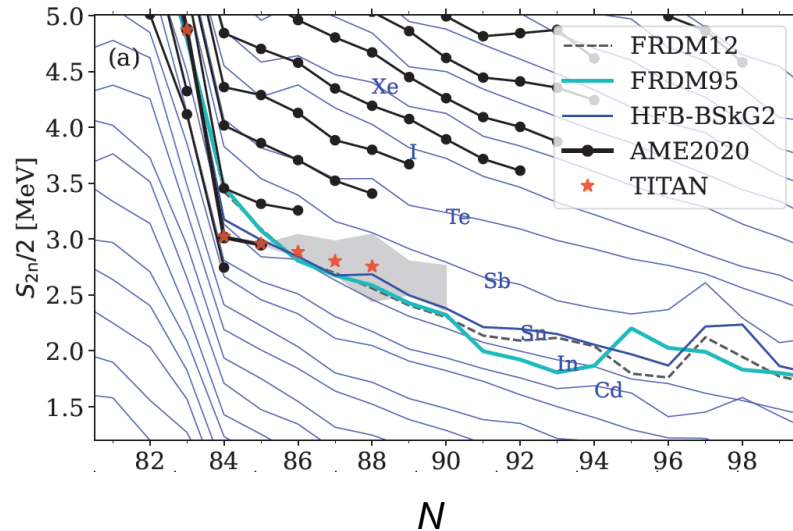


- Three-step resonant laser ionization scheme:
301.001 nm, 811.62 nm and 823.67 nm
- Cs/Ba as mass calibrants (surface ionization)

Nuclear structure beyond $N=82$

- Extend the S_{2n} beyond $N=82$ neutron shell
- Lower S_{2n} slope compared to heavier elements [shell gap Δ_{2n}]
- In agreement with the new sets of ab-initio calculations
- Possible shell closure at $N=90$ (seen in ab-initio)

A. Mollaebrahimi et al., Physical Review Letters 134 (2025), 232701

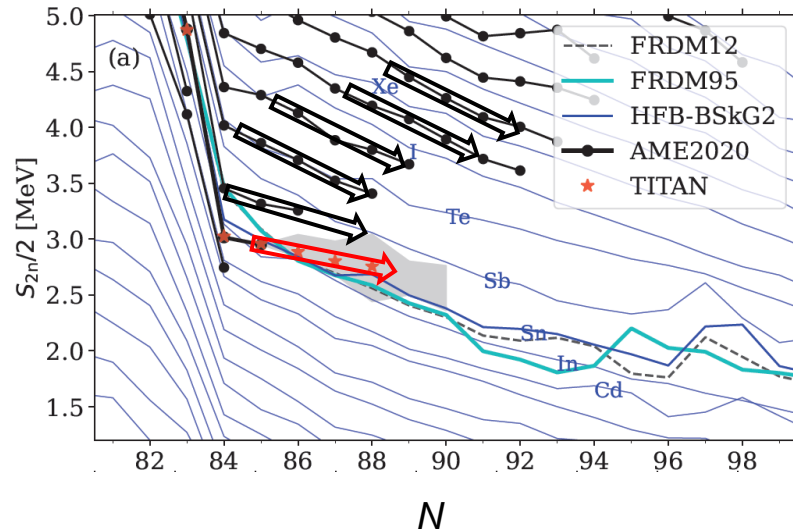


$$S_{2n} = [M(Z, A - 2) - M(Z, A) + 2M_n] \times c^2$$

Nuclear structure beyond $N=82$

- Extend the S_{2n} beyond $N=82$ neutron shell
- Lower S_{2n} slope compared to heavier elements [shell gap Δ_{2n}]
- In agreement with the new sets of ab-initio calculations
- Possible shell closure at $N=90$ (seen in ab-initio)

A. Mollaebrahimi et al., Physical Review Letters 134 (2025), 232701



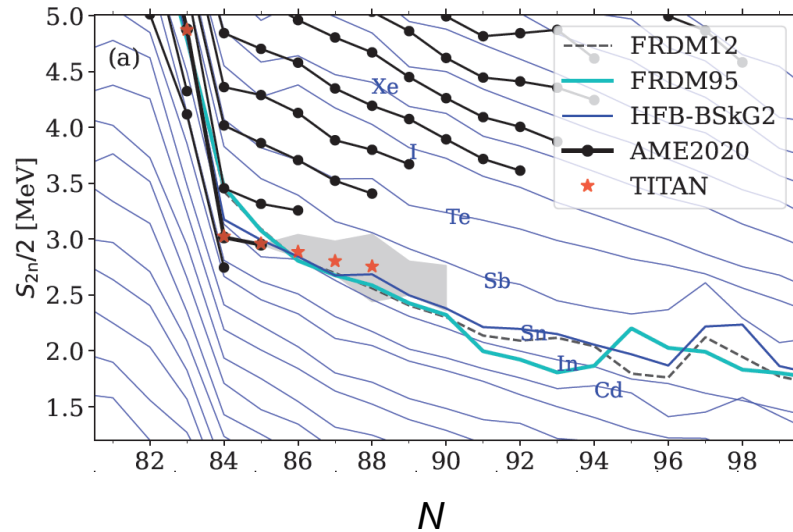
Two neutron
separation energy

$$S_{2n} = [M(Z, A - 2) - M(Z, A) + 2M_n] \times c^2$$

Nuclear structure beyond $N=82$

- Extend the S_{2n} beyond $N=82$ neutron shell
- Lower S_{2n} slope compared to heavier elements [shell gap Δ_{2n}]
- In agreement with the new sets of ab-initio calculations
- Possible shell closure at $N=90$ (seen in ab-initio)

A. Mollaebrahimi et al., Physical Review Letters 134 (2025), 232701

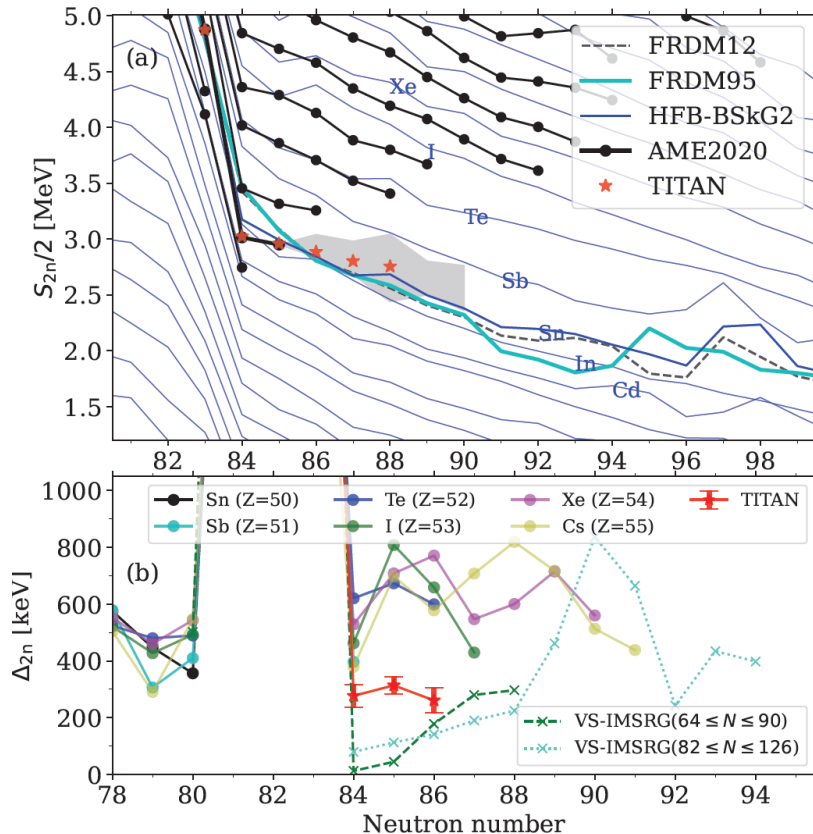


$$S_{2n} = [M(Z, A - 2) - M(Z, A) + 2M_n] \times c^2$$

Nuclear structure beyond $N=82$

- Extend the S_{2n} beyond $N=82$ neutron shell
- Lower S_{2n} slope compared to heavier elements [shell gap Δ_{2n}]
- In agreement with the new sets of ab-initio calculations
- Possible shell closure at $N=90$ (seen in ab-initio)

A. Mollaebrahimi et al., Physical Review Letters 134 (2025), 232701



Two neutron
separation energy

$$S_{2n} = [M(Z, A - 2) - M(Z, A) + 2M_n] \times c^2$$

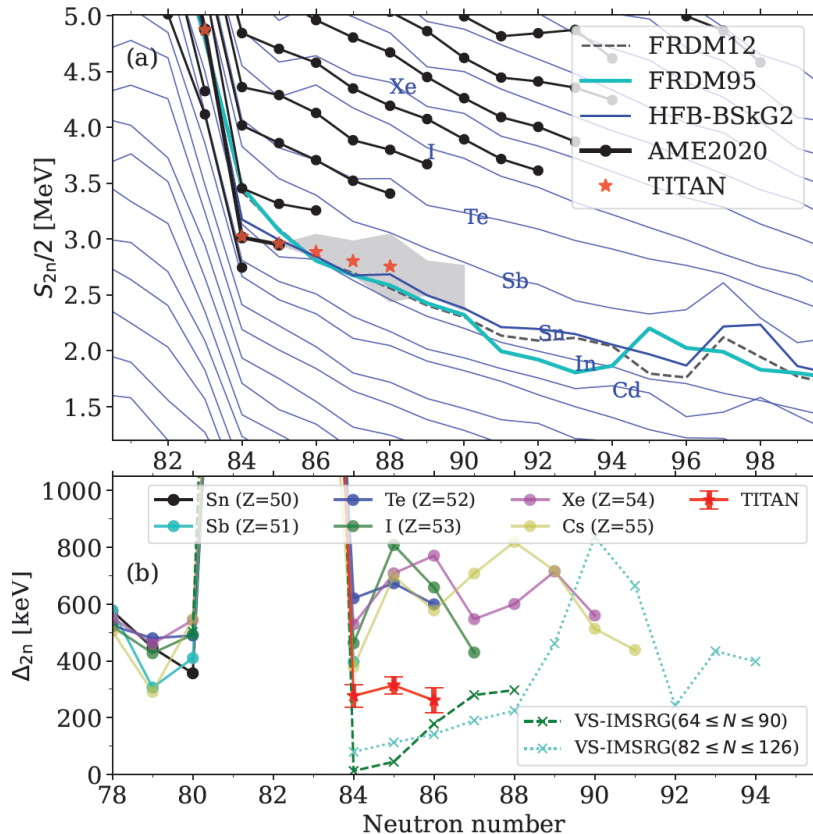
Two neutron shell gap

$$\Delta_{2n} = S_{2n}(Z, N) - S_{2n}(Z, N + 2)$$

Nuclear structure beyond $N=82$

- Extend the S_{2n} beyond $N=82$ neutron shell
- Lower S_{2n} slope compared to heavier elements [shell gap Δ_{2n}]
- In agreement with the new sets of ab-initio calculations
- Possible shell closure at $N=90$ (seen in ab-initio)

A. Mollaebrahimi et al., Physical Review Letters 134 (2025), 232701



Two neutron
separation energy

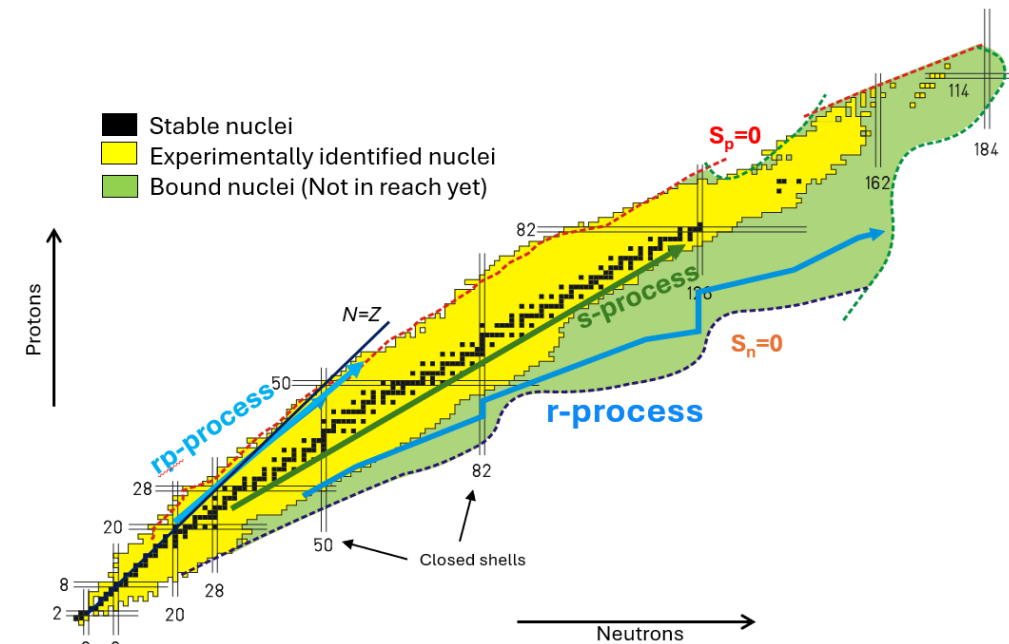
$$S_{2n} = [M(Z, A - 2) - M(Z, A) + 2M_n] \times c^2$$

Two neutron shell gap

$$\Delta_{2n} = S_{2n}(Z, N) - S_{2n}(Z, N + 2)$$

***r*-process**

- ❖ Flat trend of S_{2n} after the shell closure $N=82$
 - significant shift in the neutron drip line
 - Affecting the *r*-process path and overall abundances

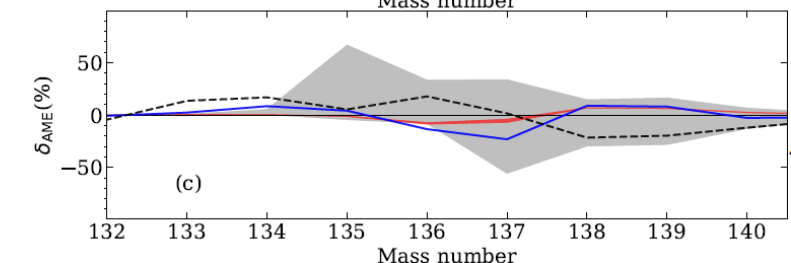
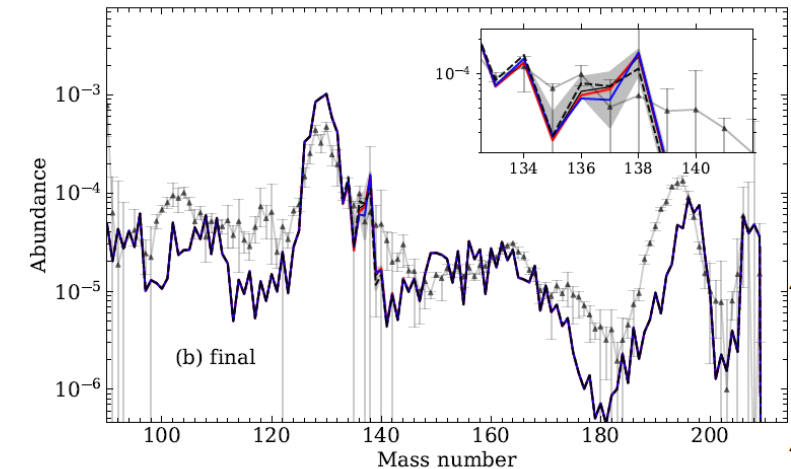
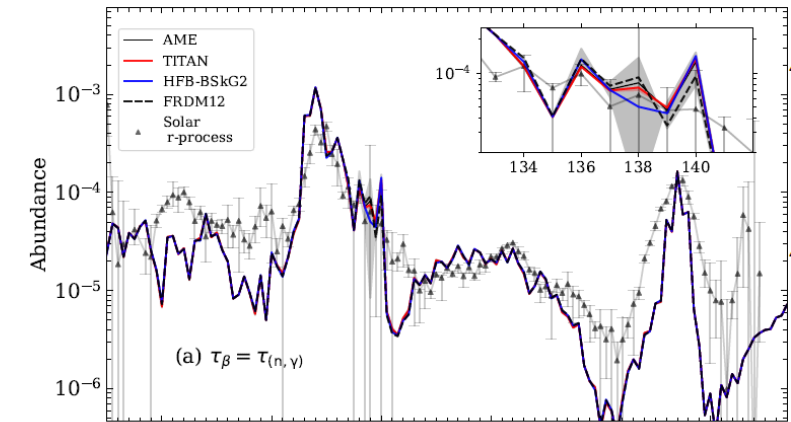


Impact on the 2nd *r*-process peak

A. Mollaebrahimi et al., Physical Review Letters 134 (2025), 232701

➤ Local effects near the 2nd peak:

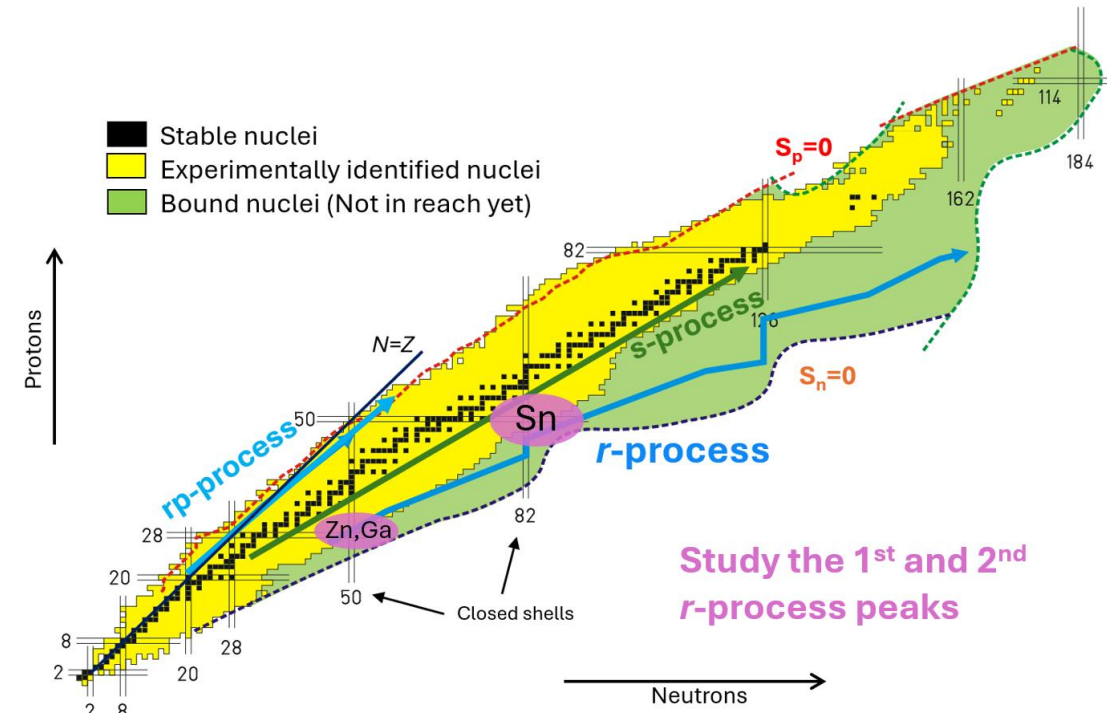
- (a) beta decays dominate over neutron capture reactions ($\tau_\beta = \tau_{n,\gamma}$)
 - AME20 uncertainty for $A=138$ spans over more than 1 order of mag.
- (b) Final abundances
 - β delayed neutron emissions at $A=138$ and $A=136$ (when decaying toward stability)
 - Uncertainty translates into $A=137$ and $A=135$
- (c) Relative difference respect to AME20
 - Large AME20 variation ($\pm 60\%$) gray band
 - Remove uncertainty by the new experimental mass values



Neutron capture rates: TALYS code
 Entropy $s = 20 k_b/\text{baryon}$
 Electron fraction $Y_e = 0.2$
 (Add 15% of material with $Y_e = 0.15$ and $s = 25 k_b/\text{baryon}$ to enhance 3rd peak)

Summary

- MR-TOF-MS setup at TRIUMF with a great capabilities for mass measurements of exotic nuclei
- Production of neutron-rich nuclei to study the 1st and 2nd *r*-process peaks
- Mass measurements of $^{79-83}\text{Zn}$, $^{79\text{m}}\text{Zn}$ and $^{85-86}\text{Ga}$
- Mass measurements of neutron-rich $^{131-138}\text{Sn}$ isotopes



MR-TOF-MS Students and Post-docs:

2016



2017



2018 - 2019



2024

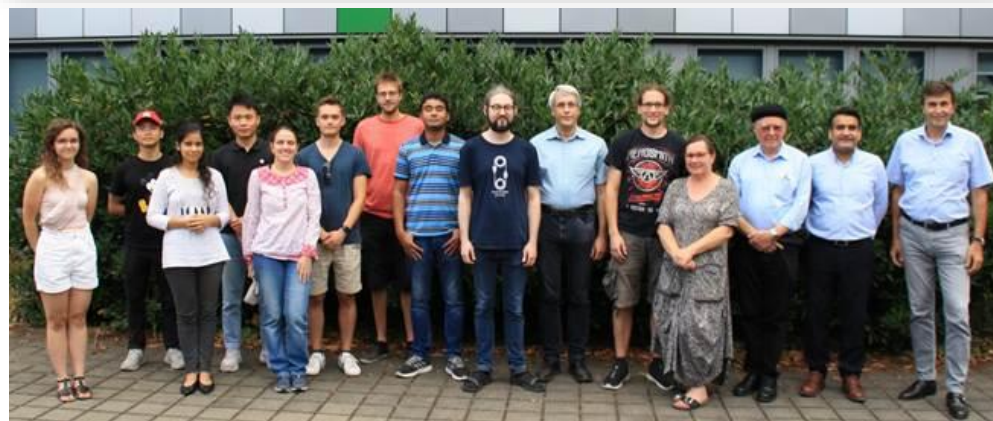


2021



Thanks!

On behalf of TITAN's Collaboration



IONAS group
JLU-Giessen